

THE CARINA NEBULA IN X-RAYS

M. F. Corcoran^{1 2}, J. Swank², G. Rawley³, R. Petre², J. Schmitt⁴,
C. Day^{1 2}

RESUMEN

New *ROSAT* PSPC and HRI observations of the Carina Nebula region are used to examine the X-ray emission from the discrete sources as well as the diffuse hot gas in the Carina Nebula near Eta Carina. Most of the diffuse emission comes from gas at a temperature of a few million degrees, but hotter (4×10^7 K) diffuse gas in an 11 pc region around Eta Car is also detected. Eta Car shows a 3 component spectrum with temperatures of 10^6 , 6×10^6 and 4×10^7 K. A 0.1×0.2 pc shell of X-ray emitting gas around Eta Car has been resolved by the HRI, and comparison of the *Einstein* HRI and *ROSAT* HRI images supports the suggestion that the soft components originate in the shell (which is unresolved by the PSPC) while the hottest gas is produced less than an arcsec from the optical star. Spectra of the bright O stars are characterized by 2 temperature components (10^7 K and 2×10^6 K) and generally show absorption columns larger than the interstellar column. PSPC and *ROSAT* HRI observations are used to examine the L_x/L_{bol} relation for hot stars in the field through the early-B spectral class.

ABSTRACT

New *ROSAT* PSPC and HRI observations of the Carina Nebula region are used to examine the X-ray emission from the discrete sources as well as the diffuse hot gas in the Carina Nebula near Eta Carina. Most of the diffuse emission comes from gas at a temperature of a few million degrees, but hotter (4×10^7 K) diffuse gas in an 11 pc region around Eta Car is also detected. Eta Car shows a 3 component spectrum with temperatures of 10^6 , 6×10^6 and 4×10^7 K. A 0.1×0.2 pc shell of X-ray emitting gas around Eta Car has been resolved by the HRI, and comparison of the *Einstein* HRI and *ROSAT* HRI images supports the suggestion that the soft components originate in the shell (which is unresolved by the PSPC) while the hottest gas is produced less than an arcsec from the optical star. Spectra of the bright O stars are characterized by 2 temperature components (10^7 K and 2×10^6 K) and generally show absorption columns larger than the interstellar column. PSPC and *ROSAT* HRI observations are used to examine the L_x/L_{bol} relation for hot stars in the field through the early-B spectral class.

Key words: nebula: individual — X-rays: sources — stars:

1. INTRODUCTION

The Carina Nebula region is one of the most interesting massive star forming regions of the Galaxy, containing bright nebulosities, faint dust lanes, open clusters with dozens of massive hot stars in various evolutionary stages (including 6 O3 stars and 3 Wolf-Rayet stars), and the peculiar object Eta Car. Eta Car is surrounded by a nebulosity called the homunculus which apparently was ejected from the star during an eruptive event in the 1840s. The nature of Eta Car is unknown but the star is generally thought to be a single very massive star close to the Humphreys-Davidson instability limit (Davidson 1971) although binary and multiple-star scenarios have also been proposed (Warren-Smith et al. 1979).

Observation of the Carina Nebula region with early non-imaging X-ray detectors (*OSO-8*, Becker et al. 1976, *Uhuru*, Forman et al. 1978) revealed at least one source of X-rays, and indicated the presence of a hard component at a temperature of a few keV. Observation with the imaging instruments on the *Einstein* Observatory (Seward et al. 1979, Seward and Chlebowski 1982, Chlebowski et al. 1984) showed various contributors to the X-ray flux: point source emission from the hot stars, point source and extended emission from Eta Car, and soft emission from a diffuse component generally associated with the optical nebulosities. The diffuse emission and the emission from most of the hot stars is produced by a thermal plasma of temperature near 1 keV. Eta Car however showed a complex, multi-temperature spectrum. Spectra of Eta Car obtained with the IPC and the SSS (Chlebowski et al. 1984) detected thermal emission at temperatures of a few hundred eV and 4 keV, which indicated that at least some of the high temperature emission observed by *OSO-8* and *Uhuru* originated very near Eta Car. A more recent *Ginga* observation (Koyama et al. 1990) of the Carina Nebula region determined a temperature for the hot gas of 4.1 keV, while a comparison of the *Ginga* and SSS fluxes suggested that some of the hot emission originated over an extended region of a few tenths of a degree in size. The Carina Nebula was also the target of a BBXRT pointing, which provided the first moderate resolution measure of the iron line region.

2. THE *ROSAT* OBSERVATIONS

The Carina Nebula was observed by both the PSPC and the HRI on *ROSAT*. The PSPC observations took place in June and December 1992 for a total of 37 ksec. The HRI observation in hand consists of a 12 ksec observation obtained in July 92. Another 38 ksec of HRI time awaits scheduling and processing. The purpose of these observations was to determine temperature variations in the diffuse emission, to determine the extent of the 4 keV component, to examine the X-ray luminosity function of the hot stars and look for variability in the point sources, and to resolve the extent and spectral distribution of the hot gas in and around Eta Car. The PSPC greyscale image is shown in Fig. 1.

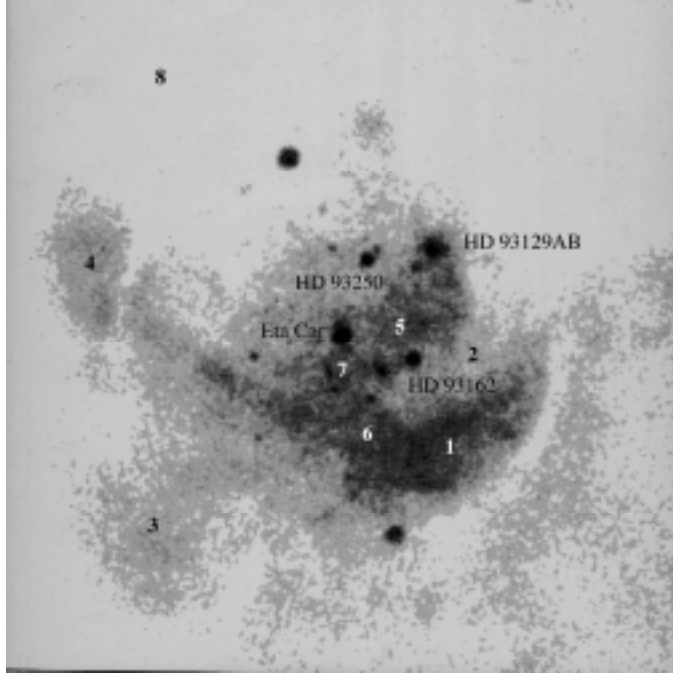


Figure 1. PSPC image of Eta Car. North is to the top, east to the left. Several bright stars and diffuse emission are apparent. Bright stars and regions of diffuse emission used in the spectral analysis are marked.

3. ANALYSIS OF THE DIFFUSE EMISSION

We extracted spectra from 7 regions within the diffuse emission indicated in Fig. 1. We used the spectrum from region 8 (which is outside most of the diffuse emission) as a measure of the background (a combination of scattered solar X-rays, charged particles and cosmic background not associated with the Carina

nebula). We modeled the spectrum from region 8 and included this model as a fixed background component in our spectral modeling of the other 7 regions. Derived temperatures, columns and emission measures are given in Table 1. The average number density n is $n = \sqrt{EM/V}$, where EM is the emission measure and V is the volume of the hot gas. Because we do not know the depth of the hot gas along the line of sight, the volume of the hot gas is not known and thus we cannot determine the density of the hot gas accurately. In order to crudely estimate densities, we assumed that the hot gas uniformly filled the volume obtained by revolving the spectral extraction region (which was either a circular or elliptical region) around one axis. The derived densities are given in table 1.

Table 1. Analysis of Diffuse Emission Spectra.

#	N_H	Log(T)	Log(EM)	Density	Surface Brightness	$\chi^2/Nbins$
	(10^{22} cm^{-2})	(K)	(cm^{-3})	(cm^{-3})	cgs	
1	0.26	6.62	56.82	0.66	1.38E-13	57/33
2	0.45	6.37	56.85	0.90	3.11E-14	28/33
3	0.64	6.21	58.11	2.67	4.61E-14	31/33
4	0.63	6.43	57.32	1.08	4.94E-14	43/33
5	0.76	6.21	57.94	7.17	8.02E-14	46/34
6	0.20	6.62	56.18	0.72	9.97E-14	35/33
7	0.56	6.43	58.08	0.62	9.59E-14	219/33

Most regions were adequately fit by 1 temperature models with a temperature of a few million degrees. An exception to this is region 7, a 7 arcmin radius circle centered near Eta Car (which excluded Eta Car, HD 93162, HD 93204 and HD93205) which required an additional hot component with $T \approx 4.1E7$ K. Thus the PSPC confirms the presence of very hot gas in an extended region of radius at least 7 arc minutes (11 pc at the distance of the Carina Nebula, taken as 2600 pc). However, the surface brightness we derive by extrapolating the ROSAT spectrum into the 2-10 keV Ginga band is 9.3×10^{-14} ergs s⁻¹ cm⁻² arcmin⁻² which is almost a factor of 2 smaller than the Ginga value (1.6×10^{-13} ergs s⁻¹ cm⁻² arcmin⁻²). However, this discrepancy may be due to uncertainties in the extrapolation of the ROSAT spectrum to the Ginga bandpass. Alternatively it may indicate that other regions of high temperature gas exist beyond the vicinity of Eta Car.

4. X-RAY EMISSION FROM ETA CAR

4.1 The Broad-Band X-ray Spectrum of Eta Car

The *Einstein* SSS spectrum of a region centered on Eta Car by Chlebowski et al. was fit by at least 2 thermal components, a soft, unabsorbed component ($T=4 \times 10^6$ K, $N_H = 2 \times 10^{21}$) and a hard, absorbed component ($T \approx 8 \times 10^7$ K, $N_H = 5 \times 10^{22}$). Observations with non-imaging detectors (OSO-8, MPC, *Ginga*) also detected the presence of Fe K-line emission near 7 keV. Our PSPC data, used in conjunction with other publically available observations at higher energies, could be used to examine the nature of the X-ray spectrum from Eta Car and the origin of the Fe line emission. We extracted a spectrum in a 2 arcmin radius circle around Eta Car from the PSPC observation. We extracted a background spectrum in a 2 arcmin annulus centered around Eta Car, excluding less luminous point sources which happened to fall in the extraction region. In order to extend the bandpass to higher energies, we also extracted source and background spectra from a public-domain IPC observation (sequence number 776) using the same source and background regions. We also examined the spectrum of the Eta Car region as observed by the SSS, in the hopes of providing improved spectral resolution. However, we found that we were unable to simultaneously fit the SSS and net PSPC and IPC spectra. This is most likely due to the contamination of the SSS spectrum by the X-ray background around Eta Car which fell within the 6 arcmin diameter field-of-view of the SSS. An estimate of the background contamination in the SSS field-of-view could be made from the IPC data, as was done by Chlebowski et al. in their analysis. We preferred to take a different, complementary approach. We used the background-corrected PSPC spectrum and the background-corrected IPC spectrum to define the source spectrum from 0.1–4.5 keV, the combined PSPC-IPC energy bands. We then used the BBXRT spectrum of Eta Car to define the high energy ($E > 4$ keV) part of the spectrum and to provide a moderately-resolved spectrum of the Fe line region near 7 keV. Because BBXRT had only crude imaging capabilities, no real background correction could be made for these data; however, the diffuse

We performed a simultaneous fit to the PSPC, IPC and truncated BBXRT spectrum using absorbed Raymond-Smith thermal spectra as the input model. Our best fit to the data required 3 thermal components, and our model χ^2 is 110 for 63 degrees of freedom. The derived parameters are given in Table 2 below, while the best fit spectrum (deconvolved from the detector responses) is shown in Figure 2. The values of N_{H} below do not include the contribution from the ISM, which was fixed near $2 \times 10^{21} \text{ cm}^2$. The unabsorbed luminosity for this model is $\text{Log } L_x = 35.55$, which is somewhat larger than the value derived by Chlebowski et al., $L_x = 2.5 \times 10^{34}$, mainly due to the larger value of N_{H} which we derive for the hottest component. Our X-ray luminosity implies $\text{Log } L_x/L_{\text{bol}} = -5.1$. This is a much higher L_x/L_{bol} ratio than is obtained for any of the other point sources in the field (§5.1).

Table 2. Best fit to Composite Eta Car Spectrum

Log (T)	Log(EM)	Log(N_{H})
7.75	58.24	23.20
6.77	56.60	21.48
6.06	57.26	—

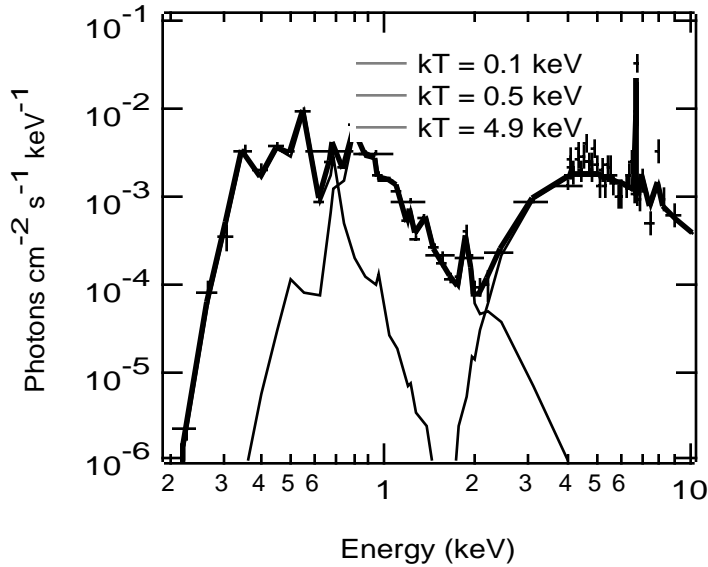


Figure 2. Eta Car 0.2-10 keV spectrum from PSPC, IPC and BBXRT observations

4.2 Extended Emission

A 15×20 arcsec (0.2×0.3 pc) shell of X-ray emitting gas surrounding the homunculus was imaged by both the *Einstein* and *ROSAT* HRI. Fig. 3 shows the *ROSAT* HRI image including optical contours of the homunculus. The X-ray shell is aligned with the axes of symmetry of the homunculus. Analysis of the Eta Car PSPC spectrum (which includes the emission from the extended shell) indicates the presence of

pc, the density of the shell is 157 cm^{-3} and the total mass in the shell is 0.01 solar mass. Fig. 3 shows a comparison of the *Einstein* and *ROSAT* HRI images. A point source of emission at the position of the optical center of light of Eta Car is apparent in the *Einstein* image but not in the *ROSAT* HRI image. This is consistent with the suggestion made by Chlebowski et al. of the existence of a hard absorbed source less than an arcsec from the location of Eta Car. Because the source is hard ($T \approx 4 \text{ keV}$) and absorbed ($N_{\text{H}} \approx 10^{22} \text{ cm}^{-2}$) it is not visible in the *ROSAT* band, which cuts off at about 2.4 keV. However, this hard source is detectable by *Einstein* since the *Einstein* bandpass extends to 4.5 keV.

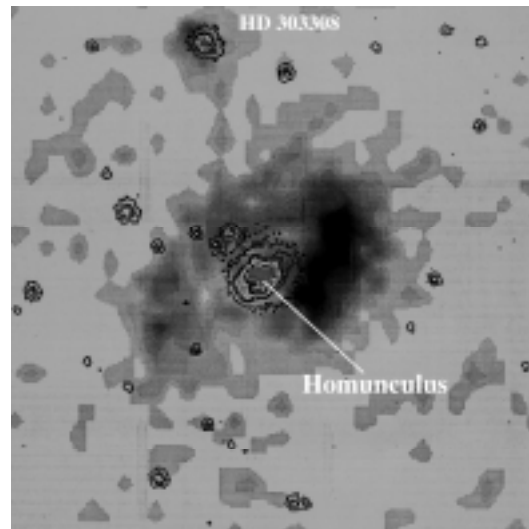


Figure 3. *ROSAT* HRI map of Eta Car and optical image of homunculus. The bright source to the northeast of the homunculus is HDE 303308 which is about 1 arcminute from Eta Car.

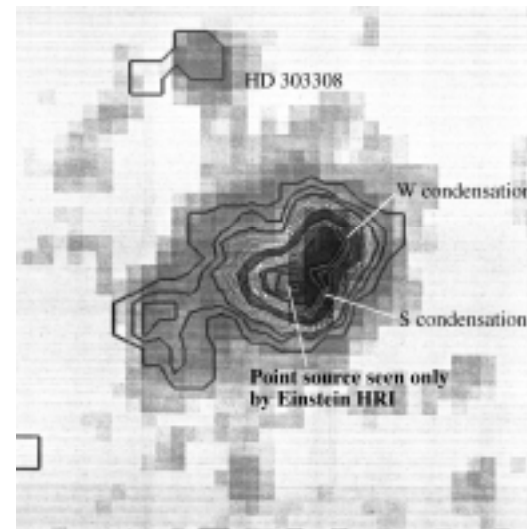


Fig. 4. *ROSAT* (greyscale) and *Einstein* (contours) HRI maps of Eta Car. The S and W condensations are sources of soft X-rays visible in both maps. The X-ray point source at the optical center of the homunculus is hard and only visible in the *Einstein* map.

5. OTHER POINT SOURCES

5.1 The X-ray Luminosity Function

We extracted counting rates for all known sources in the field of the PSPC image using the maximum-likelihood technique described by Pollock (1987). A 3×3 arcminute sub-image centered on the position of each known source was extracted from the PSPC image. The maximum likelihood technique then determines the likelihood that a point source is present above background, and if so, gives the most likely number of source and background counts in the sub-image. Source counting rates were determined by dividing the most likely number of source counts by the average value of the exposure time in the appropriate 3×3 arcminute sub-section of the merged exposure map. Positions of optical sources were obtained from the list of SIMBAD sources provided as a standard ROSAT data product. Positions from the SIMBAD list were also checked with source positions from Seward and Chlebowski (1982) for consistency.

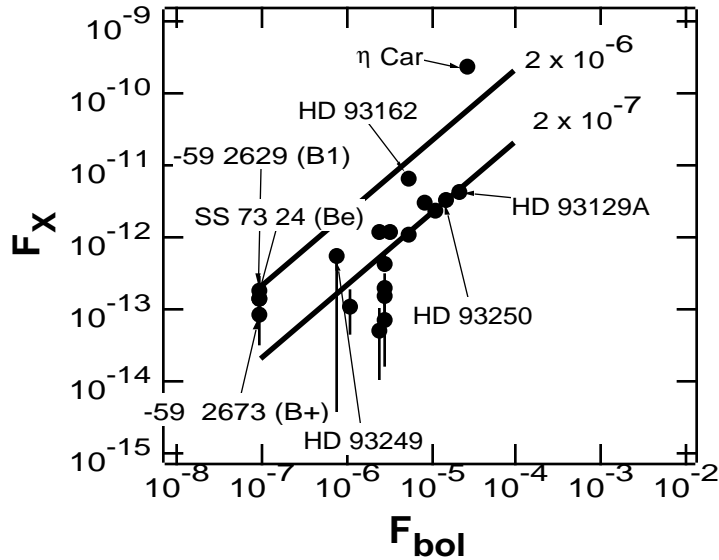


Figure 5. Dependence of F_x on F_{bol} for detected stars.

We found that the PSPC detected more than 20 stars as X-ray sources at or above the $3\text{-}\sigma$ level. The 5 brightest sources (excluding Eta Car) in the PSPC image are listed in Table 3, along with their maximum-likelihood counting rates and derived $2\text{-}\sigma$ errors. We extracted spectra for the 5 brightest sources listed in Table 3 (§ 5.3) and derived unabsorbed luminosities for all these sources and determined an energy conversion factor of $8.9(\pm 1) \times 10^{-11}$ ergs/cm²/count for these 5 stars. Assuming

that the spectra from the fainter detected sources are similar to the brightest sources, we used our derived energy conversion factor to convert from count rates to unabsorbed luminosities for the fainter sources. Figure 5 shows our derived correlation between bolometric luminosity and X-ray luminosity. In general we found that $L_x/L_{bol} \approx 2 \times 10^{-7}$, which is similar to the result obtained by Seward and Chlebowski (1982). There are some noticeable exceptions to this relation. Eta Car has the largest L_x/L_{bol} of any star in our sample. We confirm the "overluminous" nature of the WR star HD 93162 which was first noted by Seward and Chlebowski; for HD 93162, we find that $L_x/L_{bol} \approx 2 \times 10^{-6}$, similar to the value previously obtained. In addition, the PSPC observation also detected a group of X-ray bright B stars with $L_x/L_{bol} =$ a few 10^{-6} , which were not visible in the IPC pointings. However, we should point out that spectroscopic classification (and hence bolometric luminosities) are more uncertain for these stars than for the brighter stars.

5.2 X-ray Variability

X-ray lightcurves were extracted from the PSPC observation for all the stars listed in Table 2, and for Eta Car as well. No significant variability was detected in any of the bright sources at above the 10% level.

5.3 X-ray Spectral Modeling

X-ray spectra were extracted for the 5 brightest sources (excluding Eta Car) and modeled with the XSPEC software package (Eisenstein et al. 1999). The spectra were fitted with a power-law model with a

and HD 93205 a 2 component fit did not provide a good description of the data (although the 2 component fit yielded a lower value of reduced χ^2 than a single component model in these cases). Results of the spectral modeling are summarized in Table 3. We typically found temperatures of a few 10^7 K and a few 10^6 K, with absorbing columns for both the hot and cool components near but somewhat larger than the interstellar value of 2×10^{21} cm^{-2} . HD 93205 showed an exceptionally large column of 1.5×10^{22} cm^{-2} toward the hot component, but this parameter is only loosely constrained and the $1\text{-}\sigma$ lower bound on this parameter is less than 5×10^{21} cm^{-2} which is not significantly larger than the columns found for the other 4 stars in the sample. We did not find any significant correlation between mass loss rate, wind terminal velocity or wind momentum flux and the parameters (temperature, column or emission measure) of the hot gas.

Table 3. Spectral Analysis of the Bright Stars

Star	Spectral Type	PSPC rate cts s ⁻¹	NH 10 ²² cm ⁻²	Log(T) K	Log(EM) cm ⁻³	χ^2_{ν} (2T)	$\chi^2_{\nu}^1$ (1T)	Log(L_x) ² (ergs s ⁻¹)
HD93250	O3V	0.070±0.005	0.21	7.20	56.14	0.93	3.2	33.45
			0.32	6.57	56.09			
HD93129AB	O3I + O3V	0.093±0.006	0.30	7.67	56.58	1.04	4.7	33.69
			0.20	6.89	55.84			
HD93162	WN7+abs	0.288±0.007	0.41	7.30	56.73	1.48	1.9	33.76
			0.42	6.91	56.00			
HD93403	O5III	0.054±0.005	0.36	7.64	56.19	0.96	1.8	33.32
			0.22	6.96	55.85			
HD93205	O3V + O8	0.053±0.004	1.47	7.29	56.30	1.44	2.1	33.43
			0.20	6.39	55.89			

¹reduced χ^2 of best single temperature Raymond-Smith fit

² L_x has been corrected for ISM + circumstellar absorption, and is in the range 0.2—2.4 keV

6. SUMMARY

There are a distinct number of components which contribute to the X-ray emission from the Carina Nebula: point-source emission from the hot stars, a diffuse component produced by hot gas spread throughout the nebula, and emission from Eta Car. Although these components differ in the spatial distribution of the X-ray emitting gas, the physical process which produces this hot gas is similar. The hot gas is probably produced by shock heating. The currently accepted model for the production of X-rays from early-type stars is shock-heating caused by instabilities in the radiatively-driven winds these stars possess. While our data cannot conclusively prove this hypothesis, our data is consistent with it. The diffuse X-ray background which permeates this region is probably produced as large volumes of gas are driven into the

and the hardest, most absorbed emission is probably produced very close to the star as the stellar wind (at a velocity of a few thousand km/s) slams into the dust shell which surrounds the star.

However, some puzzles remain. The cause of the X-ray overluminosity of the WR star HD 93162 and the group of early B stars detected by the PSPC is unknown. In addition, while we confirm the existence of extended emission at a temperature of a few tens of millions of degrees, we cannot constrain the physical origin of this gas. Observations of this region with broad-bandpass imaging spectrometers (such as those on ASCA) are needed in order to further explore these questions and to more fully probe the dynamics of the region as measured by the X-ray emission.

REFERENCES

- Becker, R. H., et al., 1976, ApJ, 209, L68.
Chlebowski, T., et al., 1984, ApJ, 281, 665.
Davidson, K., 1971, MNRAS, 154, 415.
Forman, W., et al., 1978, ApJS, 38, 357.
Koyama, K., et al., 1990, ApJ, 362, 215.
Pollovk, A. M. T., 1987, ApJ, 320, 283.
Seward, F., and Chlebowski, T., 1982, ApJ, 256, 530.
Seward, F., et al., 199, ApJ, 234, L55.
Warren-Smith, R. F., et al., 1970, MNRAS, 187, 761.